Analysis of the Fracture Behavior of Epoxy Resins Under Impact Conditions

J. R. M. D'ALMEIDA[1] AND N. CELLA[2]

[1] Materials Science and Metallurgy Department, Pontifícia Universidade Católica do Rio de Janeiro, Rua Marquês de São Vicente,225–22453-900, Rio de Janeiro, RJ, Brazil

[2]Instituto Politécnico, UERJ, C.P. 97282, 28601–970, Nova Friburgo, RJ, Brazil

Received 23 June 1999; accepted 18 January 2000

ABSTRACT: In this work an analysis of the fracture behavior under impact of four epoxy resins was performed. The morphology of the fracture surfaces was analyzed by scanning electron microscopy and the topographic marks observed could be related to the thermal behavior of each epoxy system. The relevant properties that determine the thermal behavior were the thermal diffusivity, which was measured by using the open photoacoustic cell technique, and the glass transition temperature. As the thermal diffusivity of these materials is very low, and therefore also is their heat dissipation capacity, the impact test occurs under adiabatic conditions and a temperature increase occurs at the tip of the running cracks. Therefore, thermal blunting may occur at the crack tip and the energy absorption capacity of the resins is increased. The topographic marks observed at the fracture surface help to identify how efficient this mechanism is for each of the epoxy systems analyzed. © 2000 John Wiley & Sons, Inc. J Appl Polym Sci 77: 2486–2492, 2000

Key words: epoxy resins; impact test; thermal blunting; thermal diffusivity

INTRODUCTION

Epoxy resins are nowadays widely used in many applications that range from common adhesives and sealant to matrix in high-performance composite materials.[1,2] The outstanding versatility of this resin is due to the great reactivity of the epoxy group that can react with different compounds like aliphatic and aromatic amines, anhydrides, and polyamides.[3] The use of different hardeners produces changes on the macromolecular network of the crosslinked epoxy systems and also on the resulting macroscopic physical properties of epoxy-based materials.[4–6]

From a mechanical point of view epoxy resins are brittle materials that show very limited energy-absorbing mechanisms.[7] This picture is true even under static tests where the whole event of fracture can be thought as occurring under isothermal conditions.[8] Increasing the strain rate, such as under impact conditions, increases the tendency of materials to fail on a brittle mode. This also occurs with epoxy-based materials that show relatively low levels of energy absorption under impact. Due to the very low heat exchange capacity of polymers, one can model impact tests on these materials as an adiabatic event[8] and, therefore, new energy-consuming mechanisms could be operative, such as thermal blunting at crack tips.[9,10]

In this work a study was undertaken to verify the conditions for thermal blunting to occur. The capacity of four different epoxy-based resins to diffuse the heat generated under impact was determined and their fracture behavior was characterized. The thermal diffusivity, α, was chosen as

Correspondence to: J. R. M. d'Almeida.
Contract grant sponsor: Brazilian Agency CAPES.

Journal of Applied Polymer Science, Vol. 77, 2486–2492 (2000)

Table I Processing Parameters of the DGEBA Epoxy Systems Analyzed

Hardener	Hardener to Epoxy Ratio (phr)[a]	Cure Schedule
TETA	13	Room temperature
DDS	30	2 h at 150°C + 3 h at 220°C
DDM	27	3 h at 100°C + 2 h at 175°C
THPA/BFR	80/1	8 h at 130°C

[a] phr: parts of hardener per hundred parts of resin, in weight.

the thermal property to be evaluated because it is a key physical parameter that states how much time is needed to dissipate the heat generated at a given point inside a material. Therefore, the knowledge of α values makes it possible for the real boundary condition of the test, i.e., isothermal or adiabatic, to be correlated to the behavior shown by each of the epoxy systems analyzed. The morphology of the fracture surfaces was analyzed by scanning electron microscopy (SEM) and the topographic marks observed were correlated to the thermal behavior of each epoxy system.

EXPERIMENTAL

The samples were prepared by mixing proper quantities of a difunctional epoxy monomer, diglycidyl ether of bisphenol-A (DGEBA), respectively, with an aliphatic amine, triethylene tetramine (TETA), two aromatic poliamines, diamino diphenyl sulfone (DDS) and diamino diphenyl methane (DDM), and a mixture of the tetrahydrophtalic anhydride (THPA) and a brominated flame retardant (BFR). These four epoxy systems were fabricated by using the epoxy to harden stoichiometric ratios and the cure schedules proposed by the resin manufacturer.[11] Bulk samples of the four epoxy systems were obtained by casting the materials in bar-shaped open metal molds. Table I resumes the experimental conditions used to fabricate these epoxy systems.

Impact Charpy specimens with the average dimensions shown in Figure 1 were machined from the bars. The Charpy tests were conducted at room temperature, 23 ± .3°C, in a noninstrumented equipment with a maximum pendulum capacity of 4 J. The specimens have a notch-tip radius of 0.25 mm and the included angle of the notch tip was 45°, as specified by the ASTM standard D-256. A minimum of 10 specimens were tested per epoxy system analyzed. It is worth mentioning that even after the development of the concepts of linear elastic fracture mechanics the Charpy impact test continues to be largely used to investigate the fracture behavior of materials. When a noninstrumented equipment, as the one used here, is employed, the energy values represent the total energy consumed at the fracture event (i.e., fracture initiation and propagation). Moreover, energy losses associated with friction at mechanical parts of the test apparatus, windage of the pendulum arm, and acceleration of the test specimen contribute to the measured values. Nevertheless, if the experimental conditions are carefully maintained throughout the tests, the obtained data can be qualitatively used to compare the mechanical behavior of materials.

The fracture surfaces were analyzed by SEM. The samples were previously coated with a conducting gold-palladium film and the SEM observation was performed with secondary electrons imaging and acceleration of the electron beam ranging between 15 and 20 kV.

The thermal diffusivity was obtained by using the open photoacoustic cell (OPC) technique. Since this technique was developed,[12,13] it has been applied in the thermal and optical charac-

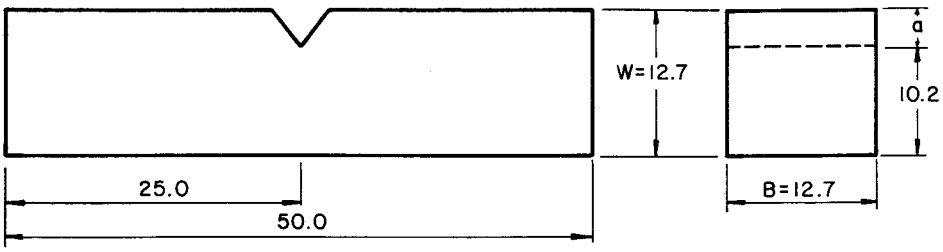

Figure 1 Geometry and dimensions of the Charpy impact test specimens.

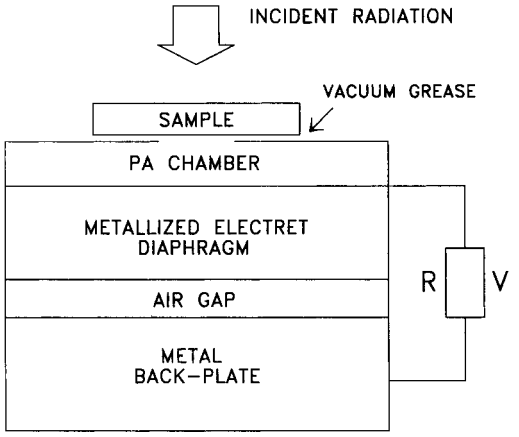

Figure 2 Schematic cross section of the open photoacoustic setup.

terization of materials, such as polymers,[14,15] glasses,[16] and plant leaves.[17,18] In contrast to the conventional photoacoustic (PA) method (for a review of photoacoustic spectroscopy, see, for example, Refs.[19] and [20]) in the OPC technique, there is no need of a transduction medium once the sample is positioned directly on the top of a commercial electret microphone. A schematic of the test apparatus is shown in Figure 2. The incident radiation is mechanically modulated and as a result of the periodic heating of the sample due to nonradiative deexcitation processes, a periodic heat flow flows from the sample to the front air chamber of the electret microphone. This periodic heat flow produces an acoustic wave at the chopping frequency, causing a deflection on the diaphragm of the microphone, which generates a voltage (V), across the resistor (R) (Fig. 2). This voltage is subsequently fed into a field effect transistor (FET) preamplifier already built into the microphone capsule. The amplitude and phase of this OPC signal is analyzed by a lock-in amplifier. Therefore, the way the light is absorbed by the sample and how the heat flows in the sample will affect the OPC signal. It means that when the OPC signal is analyzed with wavelength dependency and/or modulation-frequency dependency, the thermal and optical properties of the sample can be studied. It has been shown that the OPC signal generated is quite complex.[17] However, for limiting cases it becomes less difficult to be analyzed. When the light is absorbed at the surface of the sample (i.e., the sample is optically opaque) and the length of the thermal diffusion is shorter than the thickness of the sample (that is, it is thermally thick), the OPC signal, V_{OPC}, can be written as[16]:

$$V_{OPC} = (A/f)\exp(-af^{1/2}) \quad (1)$$

where A is a coefficient related to all parameters that affect the OPC signal but stay constant with the modulation-frequency variation, f is the modulation frequency, and $a = [(\pi l^2)/\alpha]^{1/2}$ is the coefficient related to the thermal diffusivity of the sample. In the above expression, l is the sample thickness and α the thermal diffusivity. Therefore, from a scanning in the modulation frequency, one gets an OPC signal variation as given by eq. (1). In Figure 3, an example is given of this dependence for one of the samples studied. Fitting the experimental data by using eq. (1), the coefficient a can be obtained and, then, if the thickness of the sample is known, the thermal diffusivity of the sample is obtained.

As the samples used in this work are not optically opaque, a thin aluminum foil with 12 μm of thickness was glued to the surface of the sample with help of a very thin layer of thermal past. Therefore, the light is absorbed by the aluminum foil and the heat generated is instantly transmitted to the sample.[14] For the modulation-frequency range used, 8 Hz $< f <$ 50 Hz, this approach does not disturb the theoretical model and the boundary condition of the heat generation at the surface of the sample is satisfied.[16]

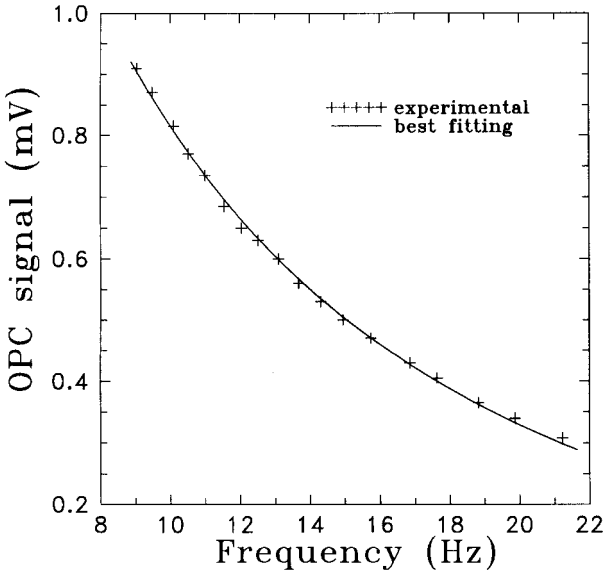

Figure 3 OPC signal amplitude as a function of the modulation frequency for the DGEBA–TETA sample. The sample thickness was 170 ± 7 μm. The solid line is the best fitting of eq. (1).

Table II Experimental Values of the Energy Absorbed at the Impact Tests (U) and from the Thermal Diffusivity Measurements (α) (The T_g values of the epoxy systems analyzed are also shown)

Hardener	U (kJ/m^2)	α (10^{-3} cm^2/s)	T_g (°C)	ΔT (°C)
TETA	2.09 ± 0.08	1.60 ± 0.13	120[a]	42
DDS	3.72 ± 1.16	1.47 ± 0.10	220[b]	140
DDM	4.65 ± 0.93	1.60 ± 0.12	184[b]	197
THPA	1.94 ± 0.85	1.44 ± 0.11	~ 150[c]	33

[a] Ref. 31.
[b] Ref. 32.
[c] Based on the cure schedule recommended by the resin manufacturer, Ref. 11.

RESULTS AND DISCUSSION

The experimental results obtained by the Charpy impact tests are shown in Table II. One can see that the epoxy systems with aromatic hardener (DDS and DDM) absorb more energy than the aliphatic and the anhydride hardener systems (TETA and THPA, respectively). Figure 4 shows the topographic marks generated at the fracture surface of the epoxy–DDM system. These topographic marks are characteristic of the discontinuous fracture event common to thermoset resins,[21] where a main-crack front intersects secondary cracks nucleated ahead of the main crack. Although varying in extension for each epoxy monomer/hardener pair, the topographic marks observed in Figure 4 are representative of the fracture surface morphology of all the epoxy systems analyzed. In Figure 4 one can see a mirror featureless zone adjacent to the crack initiation point. The mirror zone is followed by the transition and final propagation zones. These two last regions are characterized by a steady increase on the surface roughness and by the presence of conic marks.[6,21] Of prime interest for the understanding of the fracture event of a thermoset polymer is also the observation of the edges joining the conic marks. The edges can be abrupt or can show incipient deformation marks or detached striations. The presence of striations indicates a better deformation capacity of the material.[22,23]

None of the systems analyzed here exhibited the formation of striations. Nevertheless, incipient deformation marks can be seen at the fracture surfaces of the aromatic hardener epoxy systems. Figure 5(a,b) shows these marks for the DDM and DDS systems, respectively. Although the same deformation mechanism is operating for both systems, one can see that the marks developed at the fracture surface of the DDS system are more spread and shallow than the ones for the DDM system [Fig. 5(b) versus 5(a)].

Incipient deformation marks could also be seen for the DGEBA–TETA epoxy system, as shown in Figure 6. For this epoxy system, nevertheless, the edges between the topographic marks are sharp. Therefore, less energy was consumed by cooperative plastic deformation.[24] The presence of deformation marks at the fracture surface of THPA epoxy system was barely seen. For this system, one could see smooth steps and well-formed conic marks at the final propagation zone (Fig. 7). From the above discussions, one can see that more deformation mechanisms are acting at the epoxy–aromatic hardeners formulations.

The results obtained for the thermal diffusivity measurements are also shown in Table II. One can see that the values are roughly equal and, as a first approximation, one can say that they are the same for all four epoxy systems. The low values of the thermal diffusivity of these systems is a direct picture that the macromolecular network developed is not well organized for heat propagation and that the heat generated by the impact test will be dissipated very slowly. Therefore, under an impact event, a localized temperature rise

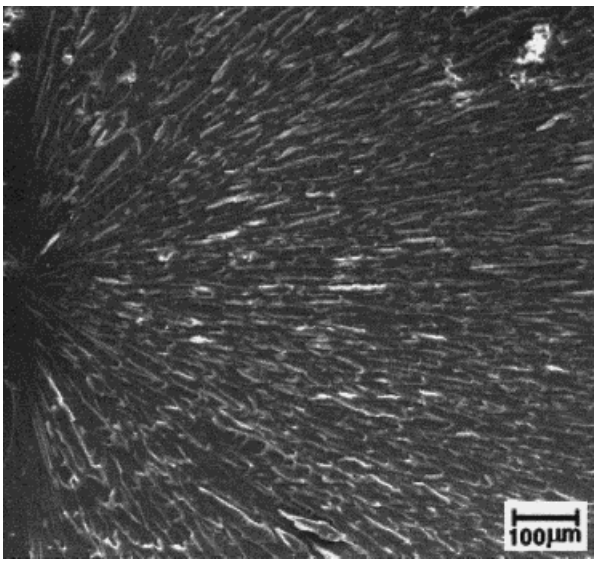

Figure 4 Overall aspects of the fracture surface of thermoset polymers. One can see a mirror flat zone surrounded by regions with conic marks. Epoxy–DDM system.

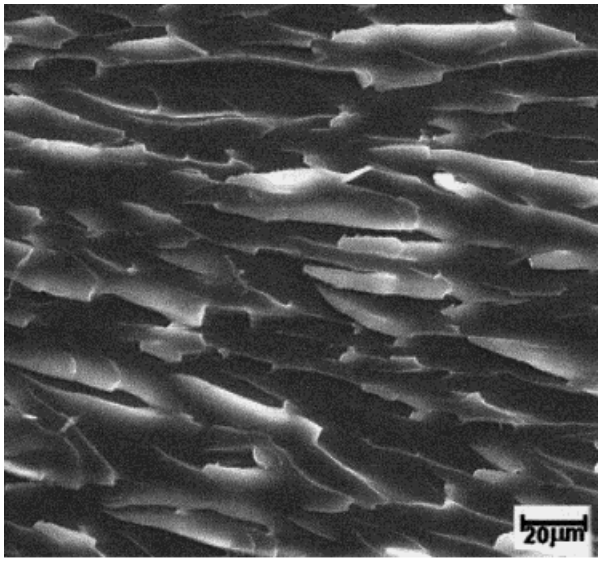

(a)

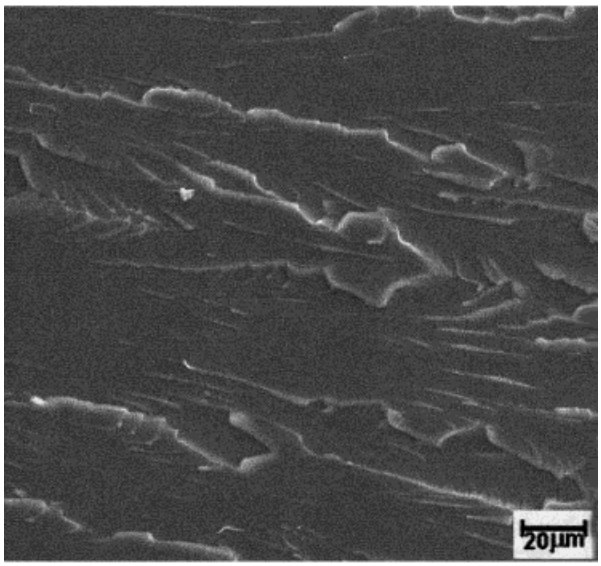

(b)

Figure 5 Deformation marks observed for (a) epoxy–DDM system; (b) epoxy–DDS system.

could take place. In other words, the impact test could occur under adiabatic conditions.

An estimation of the temperature rise at the crack tip can be done by using the equation[9,25]:

$$\Delta T = G_{Ic}/(\pi \rho c k t)^{1/2} \quad (2)$$

where G_{Ic} is the critical strain energy release rate, ρ is the density, c is the specific heat, k is the thermal conductivity, and t is the duration of the

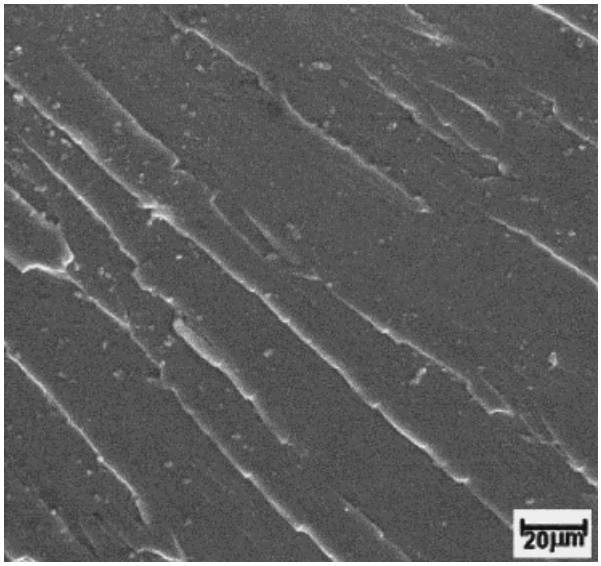

Figure 6 Topographic aspects of the incipient deformation marks developed at the fracture surface of the epoxy–TETA system.

impact event. The values of the thermal conductivity, k, were obtained by using the results of the thermal diffusivity, α. As the thermal conductivity is defined as $k = \alpha\rho c$ and the density, ρ, and the specific heat, c, can be considered as constants,[26] k is straightforwardly related to the α values. The values of density[11] and specific heat[27] used for these calculations were 1.16 g/cm^3 and

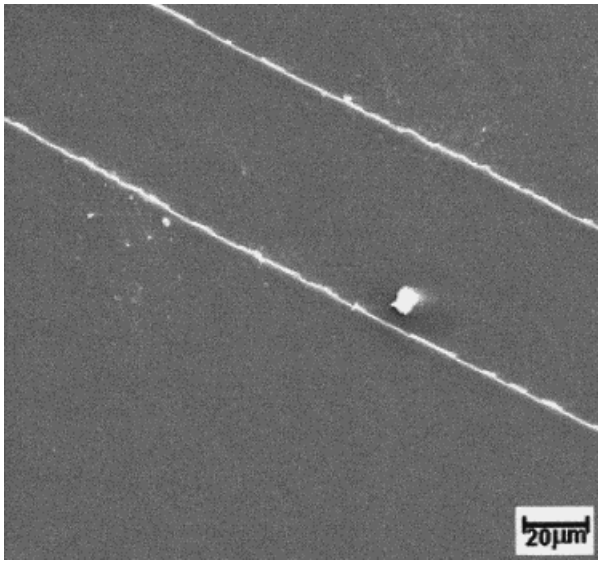

Figure 7 Sharp steps and characteristic conic marks developed at the fracture surface of brittle thermoset resins. Epoxy–THPA system.

0.40 cal/g°C, respectively. The impact time was estimated to be ≈ 1 mseg.

Values of G_I can be evaluated directly from the energy, U, absorbed in a Charpy impact test by the equation[28,29]:

$$U - U_0 = GBW\phi. \quad (3)$$

where U_0 is a term related with the kinetic energy, namely

$$U_0 = \tfrac{1}{2}\pi m v^2 \quad (4)$$

where m is the mass of the specimen and v is the test velocity. The other parameters in eq. (3) are the thickness (B), and the width (W), of the test specimens and a calibration factor, ϕ. For small cracks, the calibration factor can be approximated by[30]:

$$\phi = \frac{1}{2}x + \frac{1}{18\pi} \times \frac{L}{W} \times \frac{1}{x} \quad (5)$$

where L is the test span and x is the ratio between crack length (a) and specimen width (W) (i.e., $x = a/W$) (Fig. 1).

The temperature rise, ΔT, could then be determined from eq. (2). The values obtained are shown in Table II along with the values of the glass transition temperature, T_g, of the epoxy systems, which were determined by differential scanning calorimetry[31] or taken from the literature.[11,32] It is worth mentioning here that the values of ΔT as calculated from eq. (2) have to be regarded only as rough estimates, because, as pointed out by Low and Mai,[25] direct measurements of energy in impact tests give overestimated G_{Ic} values. This fact is due to the extra work necessary for crack propagation through the plastically deformed region formed ahead of the crack tip.[9] Therefore, a proper estimation of ΔT from measured energy values would have to give consideration to this effect.

One can see that for the DGEBA–DDM system, a high temperature rise at the crack notch tip was predicted. The calculated value is high enough to bring the polymer near to its glass transition temperature, causing softening and thus enhancing the resin toughness. In fact, there exists a good relationship between the fractographic analysis and the predicted temperature rise. As shown in Figures 5–7, deformation marks were more prominent for the DDM system, decreasing in number and height toward the THPA system. In other words, as the predicted temperature rise approaches the glass transition temperature of the epoxy systems, crack blunting occurs more extensively ahead of the crack tip. The occurrence of this mechanism can be inferred by the topographic marks left at the fracture surface of the tested specimens.

CONCLUSION

The thermal diffusivity of all epoxy systems analyzed here are low and, therefore, the impact test can be modeled as occurring under adiabatic conditions. The very low capacity of heat propagation of these polymers will produce a temperature increase that can be high enough to soften the region near the crack tip. Therefore, thermal blunting increases the energy absorption capacity of these resins. The shape of the topographic marks observed at the fracture surface has a good relationship with the presence of thermal blunting and helps to identify how efficient this mechanism is for each of the epoxy systems analyzed.

The authors acknowledge financial support from the Brazilian Agency CAPES.

REFERENCES

1. Gibson, R. F. Principles of Composite Material Mechanics; McGraw-Hill: Singapore, 1994.
2. Bauer, R. S.; Corley, S. in Reference Book for Composites Technology; Lee, S. M., Ed.; Technomic: Lancaster, 1989; Chapter 4.
3. Lee, H.; Neville, K. Handbook of Epoxy Resins; McGraw-Hill: New York, 1967.
4. Morgan, R. J.; Mones, E. T. J Appl Polym Sci 1987, 33, 999.
5. Cuddihy, E.; Moacanin, J. J Polym Sci, Part A: Polym Chem 1970, 8, 1627.
6. Graça, M. L. A.; d'Almeida, J. R. M.; Darwish, F. A. I. J Braz Soc Mech Sci 1989, 11, 133.
7. Williams, J. G. Fracture Mechanics of Polymers; Wiley: Chichester, 1984.
8. Dieter, G. E. Mechanical Metallurgy; McGraw-Hill: Tokyo, 1976.
9. Williams, J. G.; Hodgkinson, J. M. Proc R Soc London, Ser A 1981, 375, 231.
10. d'Almeida, J. R. M. in Proceedings of the 1st Ibero-American Symposium on Polymers; Grupo Español de Polímeros, Ed.; Universidad de Vigo: Vigo, Spain, 1992; p 543.
11. Dow Liquid Epoxy Resins; The Dow Chemical Company: Midland, MI, 1976.

12. da Silva, M. D.; Bandeira, I. N.; Miranda, L. C. M. J Phys E: Sci Instrum 1987, 20, 1476.
13. Perondi, L. F.; Miranda, L. C. M. J Appl Phys 1987, 62, 2955.
14. Torres-Filho, A.; Leite, N. F.; Miranda, L. C. M.; Cella, N.; Vargas, H. J Appl Phys 1989, 66, 97.
15. d'Almeida, J. R. M.; Cella, N.; Monteiro, S. N.; Miranda, L. C. M. J Appl Polym Sci 1998, 69, 1335.
16. de Lima, J. C.; Cella, N.; Miranda, L. C. M.; Chying An, C.; Frazan, A. H.; Leite, N. F. Phys Rev B: Condens Matter 1992, 46, 14186.
17. Marquezini, M. V.; Cella, N.; Mansanares, A. M.; Vargas, H.; Miranda, L. C. M. Meas Sci Technol 1991, 2, 396.
18. Pereira, A. C.; Zerbetto, M.; Silva, G. C.; Vargas, H.; da Silva, W. J.; Neto, G. O.; Cella, N.; Miranda, L. C. M. Meas Sci Technol 1992, 3, 931.
19. Rosencwaig, A. Photoacoustics and Photoacoustic Spectroscopy; Wiley: New York, 1980.
20. Vargas, H.; Miranda, L. C. M. Phys Rep 1988, 161, 45.
21. Wolock, I.; Newman, S. B. in Fracture Processes in Polymeric Solids—Phenomena and Theory, Rosen, B., Ed.; Interscience: New York, 1964; pp 235–290.
22. Atsuta, M.; Turner, D. T. J Mater Sci. Lett 1982, 1, 167.
23. d'Almeida, J. R. M.; Monteiro, S. N. Polym Adv Technol 1998, 9, 216.
24. Kinloch, A. J. Metal Sci 1980, 14, 305.
25. Low, I. M.; Mai, Y. W. J Mater Sci 1989, 24, 1634.
26. Torres-Filho, A.; Perondi, L. F.; Miranda, L. C. M. J Appl Polym Sci 1988, 35, 103.
27. Lange's Handbook of Chemistry, 10th ed.; Lange, N. A., Ed.; McGraw-Hill: New York, 1967; p 874.
28. Brown, H. R. J Mater Sci 1973, 8, 941.
29. Marshall, G. P.; Williams, J. G.; Turner, C. E. J Mater Sci 1973, 8, 949.
30. Birch, M. W.; Williams, J. G. Int J Fracture 1978, 14, 69.
31. d'Almeida, J. R. M.; Cella, N.; Carvalho, R. J. J Appl Polym Sci to appear.
32. Pogany, G. A. Eur Polym J 1970, 6, 343.